



ORIGINAL ARTICLE

OPEN

Hepatic farnesoid X receptor is necessary to facilitate ductular reaction and expression of heme biosynthetic genes

Angela E. Dean¹  | Emilian Jungwirth^{2,3} | Katrin Panzitt² | Martin Wagner²  | Sayeepriyadarshini Anakk^{1,4,5}

¹Division of Nutritional Sciences, University of Illinois at Urbana-Champaign, Urbana, Illinois, USA

²Research Unit for Translational Nuclear Receptor Research, Division of Gastroenterology and Hepatology, Medical University Graz, Graz, Austria

³Institute of Biomedical Informatics, Graz University of Technology, Graz, Austria

⁴Department of Molecular and Integrative Physiology

⁵Cancer Center at Illinois, University of Illinois at Urbana-Champaign, Urbana, Illinois, USA

Correspondence

Sayeepriyadarshini Anakk, Department of Molecular and Integrative Physiology, School of Molecular and Cellular Biology, University of Illinois Urbana-Champaign, 506 S. Mathews Ave., Room 453, Urbana, IL 61801, USA.
 Email: anakk@illinois.edu

Abstract

Background: Bile, which contains bile acids, the natural ligands for farnesoid x receptor (FXR), moves from the liver to the intestine through bile ducts. Ductular reaction often occurs during biliary obstruction. A subset of patients with erythropoietic protoporphyria, an inherited genetic mutation in heme biosynthetic enzyme ferrochelatase, accumulate porphyrin-containing bile plugs, leading to cholestasis. Here, we examined the link between FXR, bile plug formation, and how heme biosynthesis relates to this connection.

Methods: We treated female and male wild-type and global and tissue-specific *Fxr* knockout mice with a diet containing 3,5-diethoxycarbonyl-1, 4-dihydrocollidine, an inhibitor of ferrochelatase, and examined the expression of heme biosynthetic genes. We mined FXR mouse ChIP-Seq data, performed biochemical and histological analysis, and tested HepG2 and primary human hepatocytes after treatment with obeticholic acid, an FXR agonist.

Results: We observed that hepatic but not intestinal *Fxr* loss resulted in reduced bile plugs and ductular reaction in the liver. Then, we examined if FXR plays a regulatory role in heme biosynthesis and found significantly lower porphyrin accumulation in 3,5-diethoxycarbonyl-1, 4-dihydrocollidine-fed *Fxr* knockout mice. Gene expression and FXR mouse ChIP-Seq atlas analysis revealed that FXR orchestrates the expression of multiple heme biosynthetic enzymes. Finally, human HepG2 cells and primary human hepatocytes treated with obeticholic acid, showed increased expression of several heme biosynthetic genes.

Abbreviations: ALAD, aminolevulinic acid dehydratase; ALAS1, aminolevulinic acid synthase 1; ALT, alanine aminotransaminase; AST, aspartate aminotransaminase; CAR, constitutive androstane receptor; DDC, 3,5-diethoxycarbonyl-1,4-dihydrocollidine; EPP, erythropoietic protoporphyria; FECH, ferrochelatase; *fl/fl Fxr*, flox/flox farnesoid X receptor; FXR, farnesoid X receptor; OCA, obeticholic acid; OST β , organic solute transporter β ; PGC1 α , peroxisome proliferator-activated receptor gamma coactivator 1-alpha; PXR, pregnane X receptor; UROD, uroporphyrinogen III decarboxylase; UROS, uroporphyrinogen III synthase; WT, wild type.

Supplemental Digital Content is available for this article. Direct URL citations are provided in the HTML and PDF versions of this article on the journal's website, www.hepcommjournal.com.

This is an open access article distributed under the terms of the Creative Commons Attribution-Non Commercial-No Derivatives License 4.0 (CCBY-NC-ND), where it is permissible to download and share the work provided it is properly cited. The work cannot be changed in any way or used commercially without permission from the journal.

Copyright © 2023 The Author(s). Published by Wolters Kluwer Health, Inc. on behalf of the American Association for the Study of Liver Diseases.

Conclusions: Overall, our data show that hepatic *Fxr* is necessary to maintain ductular reaction and accumulation of bile plugs. FXR can direct the expression of multiple heme biosynthetic genes. Thus, modulating FXR activity in EPP patients may help alleviate its associated liver disease.

INTRODUCTION

Bile, which consists of bile acids, bilirubin, cholesterol, and other metabolites, is formed in the liver and moved along a draining system of converging bile ducts to the duodenum.^[1] When these bile ducts are blocked, causing liver injury, morphological changes known as “ductular reaction” occur.^[2] In particular, a subset of patients with erythropoietic protoporphyria (EPP) develop severe liver injury and cholestasis from biliary obstruction.^[3,4] EPP is caused by an inherited loss-of-function mutation in the final enzyme of heme biosynthesis, ferrochelatase (*FECH*), leading to hydrophobic protoporphyrin accumulation in tissues, including the liver.^[5–7] *FECH* incorporates ferrous iron into protoporphyrin IX to form heme. The liver contributes up to 15% of heme production to support the functions of hemoglobin, myoglobin, cytochrome P450s, and other hemoproteins.^[8,9] *FECH* deficiency, modeled by ethylnitrosourea-mediated chemical mutagenesis in the *Fech^{m1Pas}* mice, resulted in the development of spontaneous bile plug formation and ductular reaction.^[10–12] These findings highlight a key role for *FECH* in maintaining proper heme generation and preventing detrimental effects on liver function from porphyrin accumulation.

Bile acids, endogenous ligands for farnesoid X receptor (FXR, NR1H4), are a major component of bile.^[1,13–16] FXR facilitates other metabolic processes outside of bile acid metabolism.^[17–21] Specifically, for heme biosynthesis, FXR-mediated control of aminolevulinic acid synthase 1 (*ALAS1*), the rate-limiting step, has been reported in humans but not in mice.^[22] Furthermore, treatments with bile acids have been shown to alleviate protoporphyrin accumulation in the liver of EPP patients and in rodent models.^[23,24] Bile acid intermediates also have been shown to regulate heme biosynthesis.^[25] Together these results suggest that bile acid signaling plays a critical role in maintaining heme biosynthesis.

An inhibitor of *FECH*, 3,5-diethoxycarbonyl-1,4-dihydrocollidine (DDC), has been an invaluable chemical tool to study both ductular reaction and cholestatic liver diseases.^[26–30] Previous literature has shown that male global *Fxr* knockout (*FxrKO*) mice do not develop bile plugs or mount a ductular reaction when subjected to chemically induced porphyria via DDC or bile duct ligation.^[31,32] Based on these observed histological

changes in the liver after DDC treatment, we investigated if there is a FXR-mediated link between heme biosynthesis and these pathomorphological changes.

In this manuscript, we focused on elucidating the role of FXR in bile plug formation and subsequent ductular reaction after DDC treatment, as well as heme biosynthesis. We used global, as well as tissue-specific, *FxrKO* mice that were provided a control diet or challenged with DDC in the diet. We examined transcript changes in several genes that encode enzymes in the heme biosynthetic pathway. Here we found that the female *FxrKO* mice have significantly reduced *Fech* expression at the basal level, thus mimicking EPP. Finally, we studied how FXR activation via obeticholic acid (OCA) treatment in human cell lines mediates transcript changes in multiple heme biosynthesis enzymes. Overall, our studies demonstrate that loss of hepatic FXR signaling decreases bile plug formation in response to DDC, resulting in reduced ductular reaction, and identified FXR consensus sequences on the promoter of multiple heme biosynthetic genes. These findings suggest that FXR plays a role in these processes and potentially in progression of liver disease in EPP patients.

METHODS

Animal use

Male and female C57BL/6 wild-type (WT), whole-body *FxrKO*, liver-specific knockout (L*FxrKO*, using *Alb-Cre*), and intestinal knockout (I*FxrKO*, using *Vil1-Cre*) were used in this study. Details for verifying genotype are in the Supplemental Materials, <http://links.lww.com/HC9/A433>. Littermate controls were used for genetic knockouts. Mice were maintained in flow cages containing corn cob bedding with companion square enrichment and kept on a 12-hour light/dark cycle in a 23°C temperature-controlled facility. Food and water were provided *ad libitum*. At 12–20 weeks of age, mice were either maintained on a chow diet (Envigo, Teklad, Madison, WI, cat no. TD-07571) or provided the same diet containing 0.1% DDC (Sigma, St. Louis, MO, cat no. 137030) for 2 weeks. The diet containing DDC was placed on the floor of the cage to ensure that mice had *ad libitum* access as they adjusted to ingesting the diet. Body mass was obtained every 2–3 days to ensure that mice were not losing over the approved amount of their mass during this study. Mice

were fasted for 4 hours prior to sacrifice from ZT0 to ZT4 (7:00 to 11:00). At sacrifice, serum and liver were collected for analysis. All experiments were approved by the Institutional Animal Care and Use Committee and the Institutional Biosafety Committee at the University of Illinois Urbana-Champaign, and the guidelines for animal care and use set by the National Institute of Health were followed. For the animal studies, all care and licensing guidelines were in accordance with ARRIVE (Animal Research: Reporting of In Vivo Experiments).

Histology

Liver tissue from WT, whole-body, and tissue-specific *Fxr*KO mice was fixed in 10% neutral buffered formalin and then stored in 70% ethanol until processing. Tissues were embedded into paraffin, and 5 μ m sections were made for staining. H&E staining was completed following standard protocols.

Immunohistochemistry for cytokeratin 19

Liver sections (5 μ m thick) from female and male WT and whole-body *Fxr*KO mice were used for cytokeratin 19 (CK19) immunohistochemistry. Experimental details and reagents are found in the Supplemental Materials, <http://links.lww.com/HC9/A433>.

Biochemical serum assays

Blood was collected retro-orbitally from each animal into serum separating tubes (Becton Dickinson and Company, Fall Lakes, NJ, cat no. 365978) and incubated at room temperature for at least 30 minutes prior to centrifugation for 3 minutes at 10,000 *g* and stored at -80°C until use. Serum was used for each biochemical assay. The assay details for each biochemical serum assay are in the Supplemental Materials, <http://links.lww.com/HC9/A433>.

Reverse transcription quantitative PCR (RT-qPCR)

RNA was isolated from frozen liver tissue using TRIzol Reagent (Invitrogen, Waltham, MA, cat no. 15596-018). Briefly, liver tissue was homogenized in 1 mL of TRIzol Reagent with 1.0 mm diameter zirconium oxide beads (Next Advance, Troy, NY) using a Bullet Blender Storm (Next Advance, Troy, NY, cat no. BBY24M) set at speed 9 for 1 minute. cDNA was made using DNase I (New England Biolabs Inc., Ipswich, MA, cat no. M0303S) and Maxima H Reverse Transcriptase (Fisher, Thermo Scientific, Middletown, VA, cat no. FEREP0743) following the manufacturers' protocols, and 60 ng of cDNA was used for

each qPCR reaction. qPCR reactions were conducted using SYBR Green and analyzed by quantifying $\Delta\Delta\text{Ct}$ using the Livak method.^[33] Mouse and human primers were used for determining gene expression (Table 1).

Western blots

Aminolevulinic acid dehydratase (ALAD) and FECH were detected in the livers of female WT and global *Fxr*KO mice. The details for quantifying total protein, experimental design, and antibody information are given in the Supplemental Materials, <http://links.lww.com/HC9/A433>.

Porphyrin assay

Total porphyrin was measured in liver samples, and the protocol details can be found in the Supplemental Materials, <http://links.lww.com/HC9/A433>.

Heme assay

Total liver heme was measured using a colorimetric heme assay kit (Sigma, St. Louis, MO, cat no. MAK316) following the manufacturer's protocol. Liver lysates were made by homogenizing the liver in RIPA buffer, the same as for total protein. Liver samples were diluted 1:4 in molecular grade water to ensure measurements were in the range of the assay. The assay reagent (200 μ L) was added to 50 μ L of lysate. Reactions were incubated at room temperature for 5 minutes and then measured at 400 nm using the BioTek Synergy 2 plate reader. Heme values were calculated compared to the calibrator provided. Total heme was normalized to total protein. The details for quantifying total protein are provided in the Supplemental Materials, <http://links.lww.com/HC9/A433>.

In vitro models

HepG2 human hepatoma cells and primary human hepatocytes were used to examine the effects of FXR agonists on the heme biosynthetic pathway, and experimental details can be found in the Supplemental Materials, <http://links.lww.com/HC9/A433>.

Statistical analysis

Statistical analysis was completed using GraphPad Prism (GraphPad Software, San Diego, CA). A 2-way ANOVA with a Sidak *post hoc* test was used for analyzing the mouse studies, where there were 2 genotypes and 2 treatments. An unpaired Student

TABLE 1 Primer sequences used for mouse and human quantitative PCR (qPCR) and chromatin immunoprecipitation qPCR

Gene	Species	Forward sequence 5'–3'	Reverse sequence 5'–3'
<i>36b4</i>	Mouse	AGATGCAGCAGATCCGCAT	GTTCTTGCCCATCAGCACC
<i>Rev-erba</i>	Mouse	ACAAGCAACATTACCAAGCTGA	CACTCCATAGTGAAGCCTGA
<i>Rev-erbb</i>	Mouse	TGTGAAGGCTGTAAGGGTTTCT	CACCGTTCTCTGTTTCATCCT
<i>Foxo1</i>	Mouse	GAGTTAGTGAGCAGGCTACAT	TTTGGACTGCTCCTCAGTTCC
<i>Nrf1</i>	Mouse	GGCTGATGGAGAGGTGGAAC	GGCTTCTGCCAGTGATGCTA
<i>Ppargc1a</i>	Mouse	GTCATTCGGGAGCTGGATGG	CAACCAGAGCAGCACACTCT
<i>Alas1</i>	Mouse	GATGCCAGGCTGTGAAATTTACT	CTGTTGCGAATCCCTTGGAT
<i>Alad</i>	Mouse	GGAGAGTTTGCCATGTTGTG	TCCTTCAGCCACTTCAACAG
<i>Hmbs</i>	Mouse	CTTCTGCAGACACCAGGGG	GTTTTCTTCCGCGGTTGTGG
<i>UrosIII</i>	Mouse	AGCAGTGAAGCTGTGTTTGG	CACAGACTTGGCATTCCATC
<i>Urod</i>	Mouse	GCTGCTTGGCATACTCACTG	GGACTCAAAGAGCTGCAATG
<i>Cpox</i>	Mouse	TTGCCATTTACTGCTATGGG	ACCACCAGTGTGTGTTACCG
<i>Ppox</i>	Mouse	TGGTCCATCTACACAAGAAGTGTAT	AGGAATTGCATAGCTGAGTCTAGTT
<i>Fech</i>	Mouse	AGGTAGGAGCCACTGTCCAC	AAAGCCCTTTGATAGCCTCA
<i>Hmox1</i>	Mouse	AACTTTCAGAAGGGTCAGGTG	TGTTGCGCTCTATCTCCTCTTC
<i>Fxra</i>	Mouse	CCTCGGAACAGAAACCTTGT	CAGTGTGGGGAAAGCAGT
<i>Shp</i>	Mouse	CGATCCTCTTCAACCCAGATG	AGGGCTCCAAGACTTCACACA
<i>Ostb</i>	Mouse	ATCCTGGCAAACAGAAATCG	GGGTCTGGCAGAAAGACAAG
<i>Krt19</i>	Mouse	ATCGTCTCGCCTCCTACTT	GCAAGTCTCGATGGTCTTAAA
<i>ALAS1</i>	Human	GGAAATGAATGCCGTGAGGAAAG	CCCTCCATCGGTTTTCACTA
<i>ALAD</i>	Human	GCCTGTGTCCCTACACCTC	GCTACCACCTGACATCCTGC
<i>HMBS</i>	Human	GAAAGCCTCGTACCCTGGC	CAAGCTCCTTGGTAAACAGGCTT
<i>UROSIII</i>	Human	GCCAAGTCAGTGTATGTGGGTTG	CACAGGTTTCTCCTTCTGTATCC
<i>UROD</i>	Human	TCTCCGACATCCTTGTGTACC	CCGTAGGCGTTCTAGGTCCT
<i>CPOX</i>	Human	AGGCTGGGGTGAGCATTCTG	GCATGAGGATTCTTGGGGTGG
<i>PPOX</i>	Human	CCATCGTTCCATATTACTGGGC	CTGGCGAATGAGTGCTGAGT
<i>FECH</i>	Human	GGAGATGTTACGACTTCCTTC	CGGACTGCTCTTGAATCTTGG
<i>PPARGC1A</i>	Human	GATGAAGACGGATTGCCCTCATT	CTGGTGCCAGTAAGAGCTTCTT
<i>FXR</i>	Human	CTCATTGAACATTCCATTACCTAC	GGACCTGCCACTTGTCTGTTA
ChIP qPCR primers			
<i>Alas1</i> promoter	Mouse	TAGAATCTAGACCAGCCCTGAG	TCCGACTCTTTCGTTGTCTG
<i>Alas2</i> promoter	Mouse	TCCGACTCTTTCGTTGTCTG	CATGTCCCTGTTGATGTCACAG
<i>Fech1</i> promoter	Mouse	ACAGGATCCCTAGTGGCTGG	GACCTGGGCATCTGATAGCTG
<i>Fech1</i> promoter	Mouse	CCCCTAAAGTCACATGCAACC	GAGGAGATATACCATCAGTCGC
<i>Uros1</i> promoter	Mouse	GGACTCCACCAGTGAGCC	GGGCCAGGACTTGACTAGG
<i>Uros2</i> promoter	Mouse	GTCCAGTGGGACTCAACCC	ATGTCGCCGTCACACTGC

t test was used for analyzing the human *in vitro* culture studies, where 2 treatments were compared. Data were reported as mean \pm SEM. *p*-values are reported for 2-way ANOVA analyses. For all other analyses and the Sidak *post hoc* test, *p*-values <0.05 are reported and noted as **p* < 0.05, ***p* < 0.01, ****p* < 0.001, *****p* < 0.0001. Between 3 and 10 mice were used for each group, and the specific *n* numbers are reported for each analysis.

All the authors had access to the study data and had reviewed and approved the final manuscript.

RESULTS

DDC-induced increase in circulating bile acids is maintained in male but not female mice lacking *Fxr*

We first treated female and male C57BL/6 WT and global *Fxr*KO mice with 0.1% DDC in the diet for 2 weeks with chow diet as the control (Figure 1A). Loss of *Fxr* expression in female and male mice was confirmed in the liver, as was reduced expression of downstream

targets, small heterodimer partner (*Shp*), and organic solute transporter β (*Ost\beta*), specifically in response to DDC (Supplemental Figure S1A–C, E–G, <http://links.lww.com/HC9/A433>).^[34–37] The cytochrome P450 family, *Cyp3a*, is known to be involved in DDC metabolism, and to ensure that DDC was metabolized in both sexes and genotypes of mice, we examined the expression of *Cyp3a11*.^[27,38,39] In both sexes and genotypes, we observed upregulation of *Cyp3a11* upon DDC treatment (Supplemental Figure S1D, H, <http://links.lww.com/HC9/A433>), suggesting that DDC is being metabolized. Body weight, hepatosomatic index (liver to body weight ratio), and serum bile acids and markers of liver damage were measured to validate the model for both sexes (Figure 1 for females, Supplemental Figure S2 for males, <http://links.lww.com/HC9/A433>). DDC treatment led to a 10%–20% loss in overall body weight in female mice (Figure 1B) and ~20% weight loss in male mice (Supplemental Figure S2A, <http://links.lww.com/HC9/A433>) regardless of genotype. Hepatosomatic index in female WT mice increased by 50% (0.04–0.06), whereas in male WT mice it increased by 75% (from 0.04 to 0.07). On the other hand, *Fxr*KO male mice did not show any change in the hepatosomatic index (~0.04; Supplemental Figure S2B, <http://links.lww.com/HC9/A433>). However, female *Fxr*KO mice showed an approximately doubled hepatosomatic index (0.04–0.08) (Figure 1C). These gross findings highlight that loss of *Fxr* may result in sexual differences in response to DDC.

To gauge the liver damage after DDC treatment, we examined multiple serum markers (bile acids, bilirubin, ALT, and AST). The large variation in serum bile acid concentrations in female *Fxr*KO mice at the basal level masked the increase after the DDC treatment, whereas a stark increase in WT female mice (up to ~500 μ M) was apparently evident (Figure 1D). WT and *Fxr*KO male mice exhibited a similar increase in serum bile acid concentrations (~400 μ M) after DDC treatment, despite *Fxr*KO mice having increased basal concentrations (Supplemental Figure S2C, <http://links.lww.com/HC9/A433>). Expectantly, DDC treatment increased total serum bilirubin approximately 5 times (2–10 mg/dL) in female WT mice whereas it increased 8-fold (~2–16 mg/dL) in *Fxr*KO female mice (Figure 1E). Although male WT and *Fxr*KO mice showed increased serum bilirubin upon DDC exposure, *Fxr*KO mice (~9 mg/dL) showed lower total bilirubin concentration than the WT mice (~15 mg/dL) after the treatment (Supplemental Figure S2D, <http://links.lww.com/HC9/A433>). Notable increases in serum ALT and AST activity upon the DDC treatment were seen in WT and *Fxr*KO mice, irrespective of the sex (Figure 1F, G, Supplemental Figure S2E, F, <http://links.lww.com/HC9/A433>). Overall, we observed increased serum markers of liver damage and uncovered sex differences in response to DDC treatment.

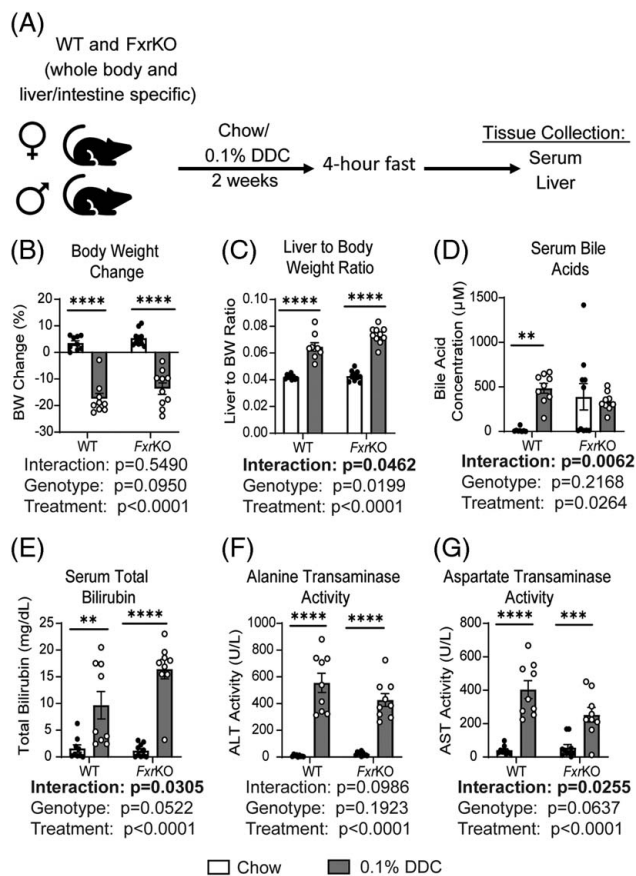


FIGURE 1 Alterations in serum liver injury markers after DDC treatment in female mice with and without *Fxr*. (A) Experimental schematic for treating female and male WT and farnesoid X receptor knockout (*Fxr*KO), along with liver (*Alb*-Cre) and intestine (*Vil1*-Cre)-specific knockouts (*LFxr*KO and *IFxr*KO, respectively), treated with 0.1% DDC for 2 weeks. (B) Body weight change and (C) liver to body weight ratio for these mice receiving chow or DDC. (D) Circulating bile acid concentration and (E) total bilirubin were measured from serum from these mice. (F, G) ALT activity AST activity were measured from serum to assess liver damage in these mice. $n = 8$ – 10 mice; mean \pm SEM; $p < 0.05$ using a 2-way ANOVA with a Sidak *post hoc* test. * $p < 0.05$, ** $p < 0.01$, *** $p < 0.001$, **** $p < 0.0001$ and are indicative of significant differences in diet within a genotype. Abbreviations: ALT, alanine aminotransaminase; AST, aspartate aminotransaminase; DDC, 3,5-diethoxycarbonyl-1,4-dihydrocollidine; WT, wild type.

Loss of *Fxr* results in reduced bile plugs and ductular reaction in the liver

Next, we examined liver histology after treatment with DDC and its respective controls. The WT animals showed bile plugs with ductular reaction, as shown by CK19+ staining and expression, a cholangiocyte marker,^[40] and inflammation (Figures 2 and 3A–C, Supplemental Figure S3A, <http://links.lww.com/HC9/A433>, Supplemental Figure S4A–C, <http://links.lww.com/HC9/A433>).^[27,30,31] Both sexes of *Fxr*KO had reduced bile plugs and lacked robust ductular reaction compared with WT animals (Figure 2A, Figure 3A–C,

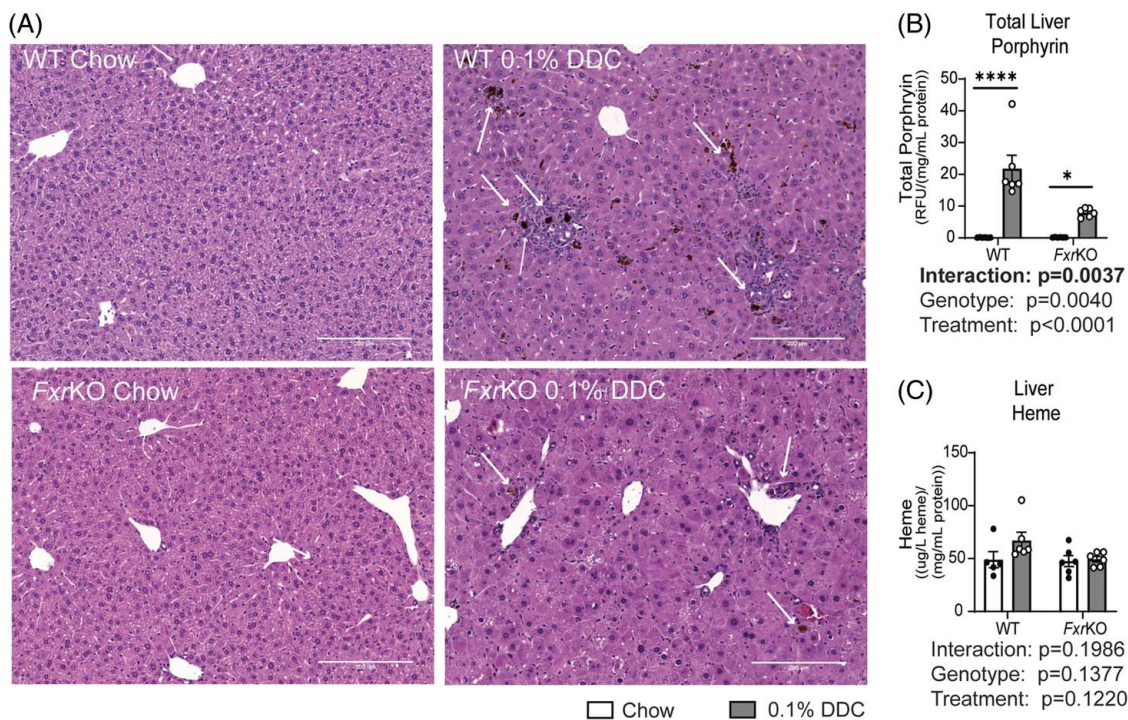


FIGURE 2 Reduced bile plugs and ductular reaction is observed in the liver of *FxrKO* female mice. (A) H&E staining for female WT and *FxrKO* C57BL/6 mice receiving either a chow diet or a diet containing 0.1% DDC for 2 weeks. White arrows indicate bile plugs (dark red) and ductular reaction. Scale is set at 200 μ m. (B) Total porphyrin and (C) total heme from the liver of experimental animals. n = 6 mice; mean \pm SEM; $p < 0.05$ using a 2-way ANOVA with a Sidak *post hoc* test. * $p < 0.05$, ** $p < 0.01$, *** $p < 0.001$, **** $p < 0.0001$ and are indicative of significant differences in diet within a genotype. Abbreviations: DDC, 3,5-diethoxycarbonyl-1,4-dihydrocollidine; *FxrKO*, *Fxr* knockout; WT, wild type.

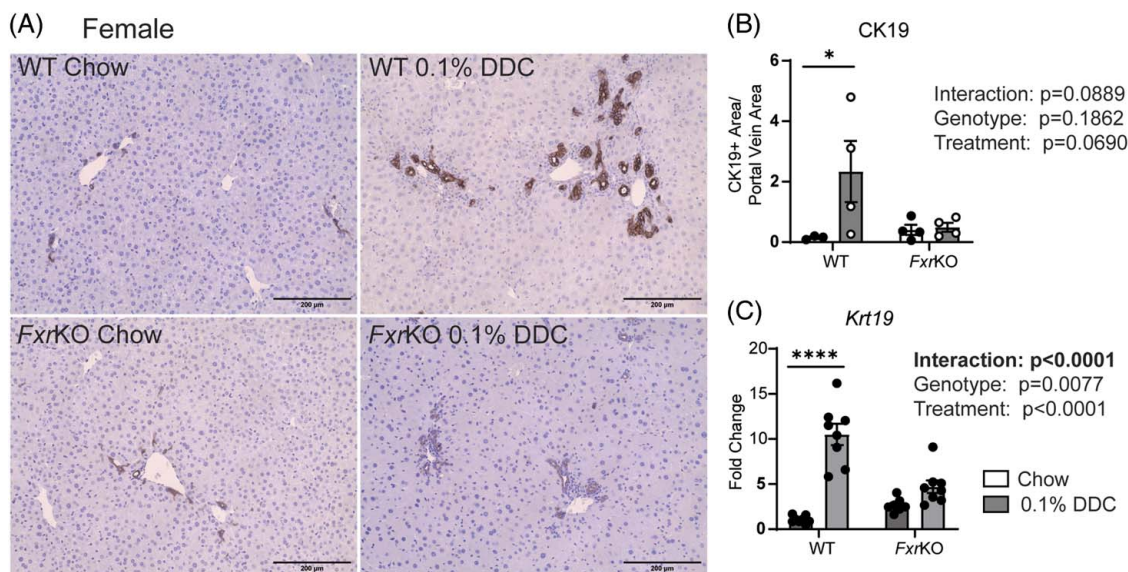


FIGURE 3 CK19+ area is reduced in female *FxrKO* mice with 0.1% DDC treatment compared with WT mice. CK19+ area in (A) female WT and *FxrKO* mice either provided a control chow diet or a diet containing 0.1% DDC for 2 weeks and quantified (B) by measuring CK19+ area in the portal field and then normalized to portal vein area using ImageJ. (C) Fold change in *Krt19* expression in corresponding livers was also measured. n = 3–7 mice; mean \pm SEM; $p < 0.05$ using a 2-way ANOVA with a Sidak *post hoc* test. * $p < 0.05$, ** $p < 0.01$, *** $p < 0.001$, **** $p < 0.0001$ and are indicative of significant differences in diet within a genotype. Abbreviations: DDC, 3,5-diethoxycarbonyl-1,4-dihydrocollidine; WT, wild type.

Supplemental Figure S3A, <http://links.lww.com/HC9/A433>, Supplemental Figure S4A–C, <http://links.lww.com/HC9/A433>), consistent with previous reports in male *Fxr*KO mice.^[31]

The H&E histology of reduced bile plug formation associated well with the lower levels of total liver porphyrin after the DDC regimen in male and female *Fxr*KO mice compared to their WT counterparts (Figure 2B, Supplemental Figure S3B, <http://links.lww.com/HC9/A433>). Despite changes in total liver porphyrin, total heme in the liver was unchanged in the females but elevated in the males, irrespective of the genotype, upon the DDC treatment (Figure 2C, Supplemental Figure S3C, <http://links.lww.com/HC9/A433>). Overall, loss of *Fxr* results in reduced bile plug formation and ductular reaction as observed histologically and by lower total porphyrin in both sexes compared to their corresponding WT controls.

Hepatic FXR is essential for DDC-mediated bile plug formation and ductular reaction

The reduced bile plugs and ductular reaction in *Fxr*KO led us to investigate if the FXR in hepatocytes or intestine was responsible for this observation. We generated *LFxr*KO with *Alb*-cre and *IFxr*KO with *Vil1*-cre in female mice. Lack of increased expression of *Fxr* targets *Shp* and *Ostβ* after the DDC treatment confirmed loss of functional FXR (Supplemental Figure S5A, B, <http://links.lww.com/HC9/A433>). Two weeks of treatment with DDC-containing diet elicited a robust ductular reaction in the control flox/flox farnesoid X receptor (*fl/fl Fxr*) and *IFxr*KO animals. However, the *LFxr*KO mice mimicked reduced bile plugs and ductular reaction seen in the global *Fxr*KO mice, indicating the need for hepatic FXR in promoting ductular reaction (Figure 4A). Despite the observed morphological differences, all 2 genotypes had 20%–30% weight loss and a similar increase in hepatosomatic index upon DDC treatment (Supplemental Figure S5C, D, <http://links.lww.com/HC9/A433>). Serum bile acid concentrations increased in control *fl/fl Fxr* mice, but concentrations were variable in *LFxr*KO and *IFxr*KO with DDC treatment, leading to no observed statistical difference ($p > 0.05$) between the groups (Figure 4B). In response to DDC, *fl/fl Fxr* and *IFxr*KO showed marked increases in liver damage markers, serum ALT, AST, and total bilirubin, while *LFxr*KO only showed a significant increase in serum ALT and total bilirubin (Figure 4C–E). Although all three groups had increased porphyrin levels in the liver upon DDC treatment, its accumulation was dampened in *LFxr*KO mice compared to the other 2 genotypes (Figure 4F). These results confirm that liver FXR is required for bile plug formation and subsequent ductular reaction in response to DDC challenge in female mice.

Alad and *Fech* have altered expression in the absence of *Fxr* in the livers of female mice

DDC inhibits FECH (the final enzyme in heme biosynthesis), but loss of *Fxr* negated the ductular reaction, so we examined if FXR regulates the expression of genes along the heme biosynthetic pathway to help explain this observed phenotype. We analyzed the transcript levels of all eight enzymes along the heme biosynthesis pathway in female and male mice (Figure 5A–I, Supplemental Figure S6, <http://links.lww.com/HC9/A433>). To gain insight into how FXR can regulate heme biosynthetic enzymes in response to DDC, we analyzed the interaction between treatment and genotype. Seven out of the eight genes were downregulated in the WT livers after the DDC treatment in female mice (Figure 5), while all 8 genes were reduced in WT male mice (Supplemental Figure S6, <http://links.lww.com/HC9/A433>). *Alas1*, the rate-limiting enzyme in heme biosynthesis, had similar expression between both genotypes and treatments in female mice (Figure 5B), which was consistent with prior literature.^[22] When FXR was deleted, we observed a basal reduction in *Fech* transcript expression in female mice, and significant interactions ($p < 0.0001$) between treatment and genotype for *Fech* and *Alad* expression in female mice (Figure 5C, I). This suggested these 2 genes may be regulated by FXR. However, other genes along the heme biosynthesis pathway showed similar responses in expression after the DDC treatment between genotypes (Figure 5D–H). Next, we tested the protein levels and found a reduction in ALAD protein after the DDC treatment only in female WT mice but not in the *Fxr*KO mice (Figure 5J, K). Despite a slight increase in FECH in WT mice, it did not hold significance, and we did not see a dramatic reduction in FECH protein in the absence of *Fxr* (Figure 5J, K). Male *Fxr*KO mice also displayed treatment and genotype interactions in *Alad* expression, similar to the gene expression pattern in female mice. In addition, *Cpox* and *Ppox* genes showed a p -value < 0.05 for the interaction between treatment and genotype (Supplemental Figure S5F, G, <http://links.lww.com/HC9/A433>), suggesting sex-dependent roles for FXR in mediating heme biosynthesis.

We then also investigated the heme biosynthesis pathway in the control *fffFxr*, *LFxr*KO, and *IFxr*KO livers. Similar to the global *Fxr*KO, we observed reduction in gene expression in 7 of the 8 genes in response to DDC in all three genotypes (Supplemental Figure S7A–H, <http://links.lww.com/HC9/A433>). All of these genes, except *ALAS1* and *Cpox*, displayed a slight increase in basal expression up to 1.5-fold due to loss of *Fxr* in the hepatocyte (Supplemental Figure S7A, F, <http://links.lww.com/HC9/A433>). This is intriguing as in the global *Fxr*KO only *Hmbs* showed a basal increase in

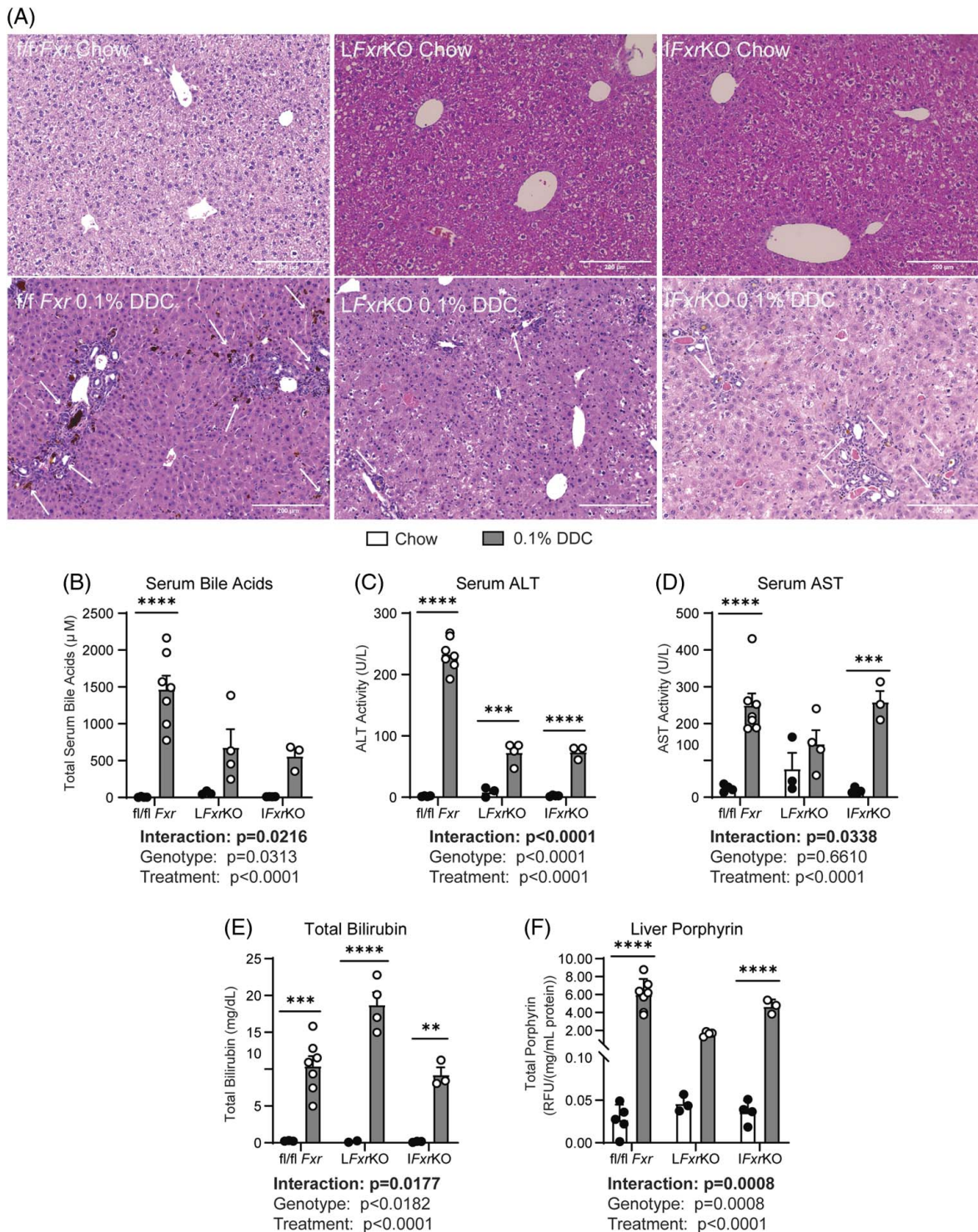


FIGURE 4 Loss of hepatic FXR results in poor ductular reaction in response to DDC in female mice. (A) H&E staining for female control fl/fl *Fxr* liver-specific *Fxr* knockout using albumin-Cre (LFxrKO), and intestine-specific *Fxr* knockout using villin1-Cre (IFxrKO) receiving either a chow diet or a diet containing 0.1% DDC for 2 weeks. White arrows are used to indicate bile plugs (dark red) and ductular reaction. Scale is set at 200 μm. (B) Circulating bile acid concentration, as well as serum markers of liver damage (C) ALT activity, (D) AST activity, and (E) total bilirubin were measured in these mice. (F) Total hepatic porphyrin was measured to examine accumulation. $n = 3-7$ mice; mean \pm SEM; $p < 0.05$ using a 2-way ANOVA with a Sidak *post hoc* test. * $p < 0.05$, ** $p < 0.01$, *** $p < 0.001$, **** $p < 0.0001$ and are indicative of significant differences in diet within a genotype. Abbreviations: ALT, alanine aminotransaminase; AST, aspartate aminotransaminase; DDC, 3,5-diethoxycarbonyl-1,4-dihydrocollidine; *Fxr*KO, *Fxr* knockout; WT, wild type.

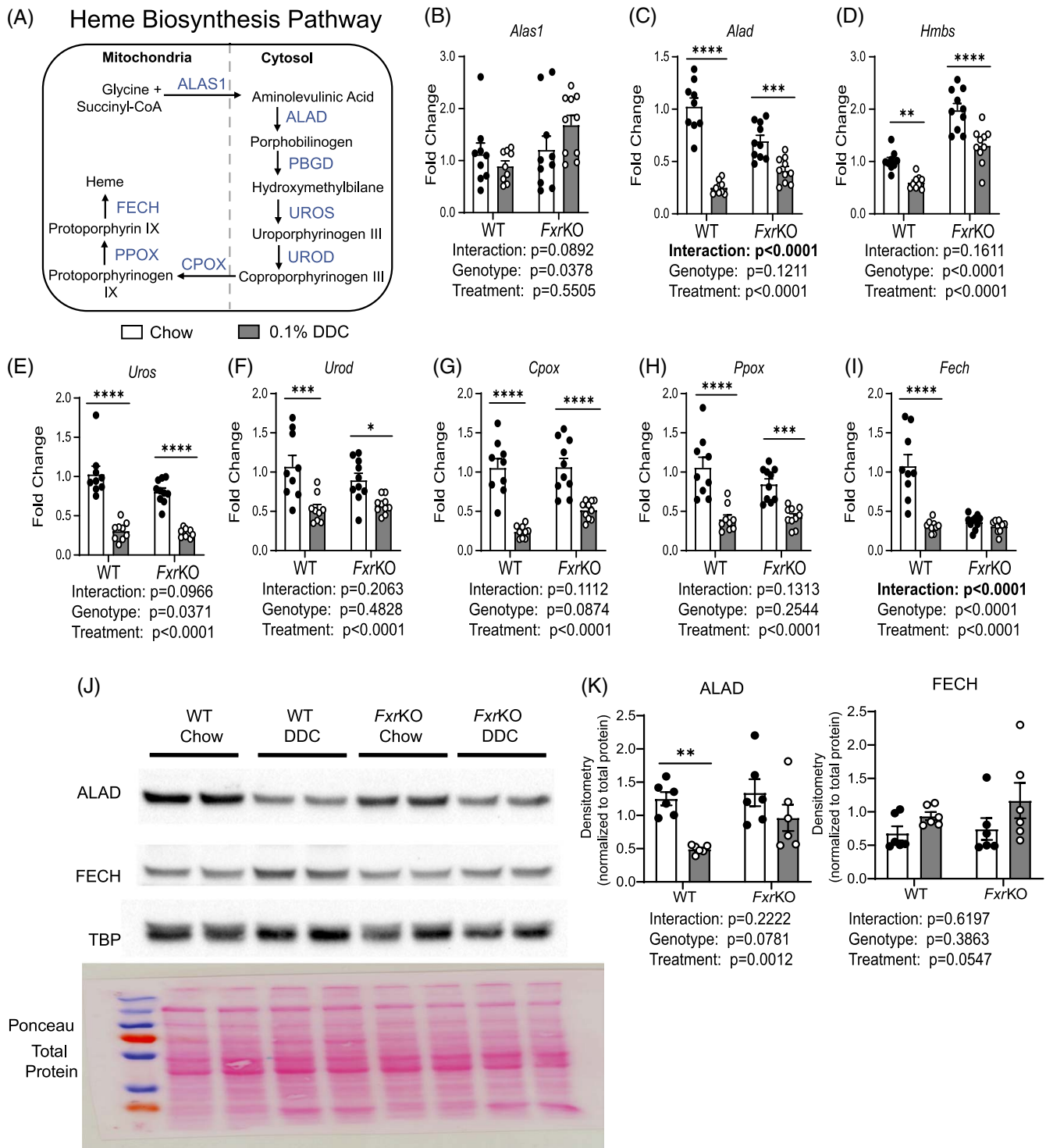


FIGURE 5 Altered expression in the absence of *Fxr* in livers of female mice. (A) Schematic of heme biosynthesis pathway in the liver. (B–I) Fold change for heme biosynthetic gene expression for WT and farnesoid X receptor (*FxrKO*) female mice on a C57BL/6 background provided a control chow diet (B) *Alas1*, (C) *Alad*, (D) *Hmbs*, (E) *Uros*, (F) *Urod*, (G) *Cpox*, (H) *Ppox*, and (I) *Fech*. (J) Representative western blot for female WT and *FxrKO* mice for ALAD and FECH. TBP was used as a loading control. Ponceau S staining shown to verify equal loading in all lanes. (K) Densitometry for ALAD and FECH from 3 separate blots normalized to total protein. Six mice per group were used for the densitometry analysis. $n = 6–10$ mice; mean \pm SEM; $p < 0.05$ using a 2-way ANOVA with a Sidak *post hoc* test. * $p < 0.05$, ** $p < 0.01$, *** $p < 0.001$, **** $p < 0.0001$ and are indicative of significant differences in diet within a genotype. Abbreviations: ALAD, aminolevulinic acid dehydratase; ALT, alanine aminotransferase; AST, aspartate aminotransferase; DDC, 3,5-diethoxycarbonyl-1,4-dihydrocollidine; FECH, ferrochelatase; *FxrKO*, *Fxr* knockout; WT, wild type.

transcript levels. Although deletion of FXR in the hepatocyte was sufficient to dampen bile plug formation and ductular reaction, we did not find decrease in *Fech* basal gene expression nor the reduction in *Alad* and *Fech* after DDC that was observed in global loss of *Fxr* in L*Fxr*KO female livers (Figure 5). These results were also not recapitulated by I*Fxr*KO mice. Nonetheless, L*Fxr*KO and *Fxr*KO showed alteration in the expression of genes in the heme pathways.

Murine heme biosynthesis genes display consensus binding sequences of FXR

To test if FXR binds and directs the transcriptional control of heme synthesis, we mined the FXR Atlas (<https://fxratlas.tugraz.at>), a curated database of mouse FXR ChIP-seq studies in the liver,^[41] to examine if any of these enzymes were downstream targets. Four of the 8 genes, *Alas1*, *Alad*, *Uros*, and *Fech*, had FXR binding peaks, indicating its recruitment to these sites (Figure 6). Of note, FXR binding to *Alad* and *Fech* is highly relevant, as these 2 genes showed changes in expression upon loss of FXR in our mouse studies. To validate these findings, we performed a FXR ChIP-PCR using livers from female WT and *Fxr*KO mice with and without DDC treatment. Although we saw binding in the FXR ChIP-seq mouse pool, we do not observe any binding of FXR to *Alas1*, *Uros*, or *Fech* above the negative control in the chow or DDC treated samples using ChIP-PCR (Supplemental Figure S8, <http://links.lww.com/HC9/A433>). FXR deletion or activation may directly control expression of genes along the heme biosynthetic pathway; however, under the context of DDC challenge, indirect FXR regulation may be linked to these observed changes.

Decreased PGC1 α signaling may lower heme biosynthetic gene expression in *Fxr*KO female livers

We then evaluated if FXR loss alters the known transcriptional regulators of heme biosynthesis. So we examined the expression of *Ppargc1a*, *Foxo1*, *Nrf1*, *Rev-erba*, and *Rev-erbb*^[43-45] in chow and DDC-fed WT or global *Fxr*KO mice of both sexes. For instance, peroxisome proliferator-activated receptor gamma coactivator 1-alpha (PGC1 α) is known to regulate *Alas1* expression by co-activation of *Foxo1* and *Nrf1*.^[43,44] As expected, DDC treatment downregulates all 3 transcripts in female WT mice. Notably, expression of *Ppargc1a* and *Foxo1* is significantly lower in female *Fxr*KO basally, so it cannot be suppressed further upon exposure to DDC (Supplemental Figure S9A, B, <http://links.lww.com/HC9/A433>). This implies that FXR

maintains basal expression of *Ppargc1a* and *Foxo1*. *Nrf1* expression is maintained irrespective of FXR expression and is repressed by DDC feeding in both genotypes (Supplemental Figure S9C, <http://links.lww.com/HC9/A433>). Nuclear receptors, *Rev-erba* and *Rev-erbb*, previously were identified to bind heme as a ligand and regulate heme biosynthesis through ALAS1 via a feedback loop.^[45] We investigated and found similar changes in expression in these nuclear receptors upon DDC treatment independent of FXR (Supplemental Figure S9D, E, <http://links.lww.com/HC9/A433> and Supplemental Figure S10D, E, <http://links.lww.com/HC9/A433>).

On the other hand, a basal reduction in *Foxo1* that is minimally responsive to DDC treatment was seen in male mice lacking *Fxr* (Supplemental Figure S10B, <http://links.lww.com/HC9/A433>). In contrast to the female mice, loss of *Fxr* in male mice does not lead to reduced basal expression of *Ppargc1a* (Supplemental Figure S10A, <http://links.lww.com/HC9/A433>). Furthermore, we see that *Nrf1* is repressed to a greater degree compared to their WT counterparts in males in response to DDC treatment (Supplemental Figure S10C, <http://links.lww.com/HC9/A433>), which in turn may alter heme biosynthesis. These results highlight sexual differences in the expression changes of known regulators of heme biosynthesis during DDC challenge upon deletion of FXR.

Apart from synthesis, we examined heme oxygenase (*Hmox1*), a gene that encodes the rate-limiting enzyme of heme catabolism,^[46] to examine heme breakdown in the different genotypes and treatments when FECH is inhibited by DDC. We observed that DDC treatment is sufficient to induce *Hmox1* transcript expression. Intriguingly, this induction in female mice is FXR-independent, whereas in males it is FXR-dependent (Supplemental Figure S9F, <http://links.lww.com/HC9/A433>, Supplemental Figure S10F, <http://links.lww.com/HC9/A433>).

Based on all these data, we posit that the male and female *Fxr*KO mice may employ distinct mechanisms to minimize bile plug formation and ductular reaction. Although reduced expression of *Ppargc1a* is common in both sexes of *Fxr*KO mice, females also have lower *Foxo1* expression, whereas males modulate *Nrf1* or *Hmox1*, which may contribute to decreased protoporphyrin accumulation, and thus, reduced ductular reaction in response to DDC.

Activation of FXR in HepG2 and primary human hepatocytes alters the expression of heme biosynthetic genes

To translate our animal studies into a human background, we treated HepG2 cells and primary human hepatocytes with the FXR ligand OCA. After OCA treatment in these

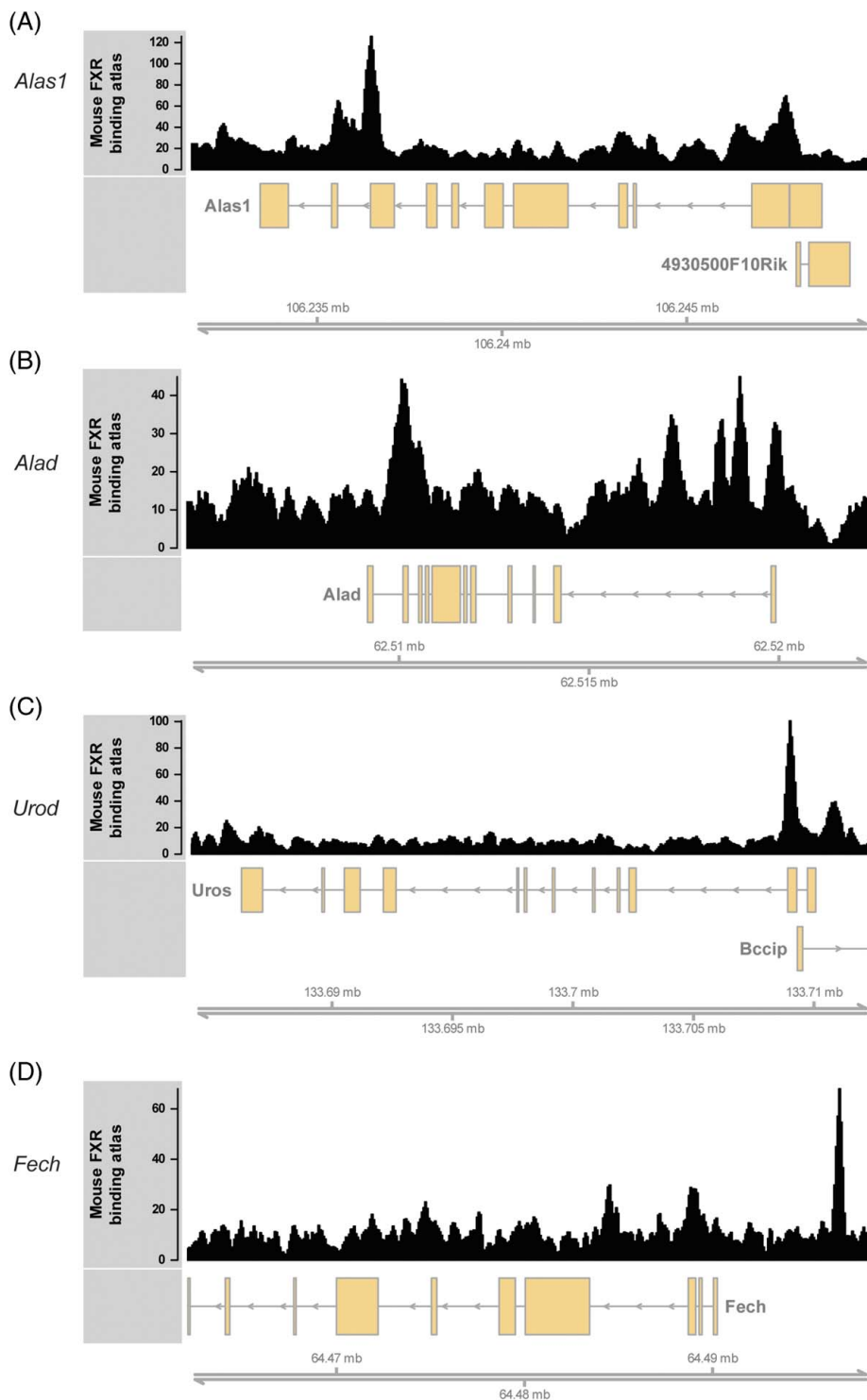


FIGURE 6 FXR consensus sequences were identified and shown to be involved in regulation of multiple heme biosynthesis genes in mice. FXR binding peaks from a compilation of CHIP-seq data sets for heme biosynthetic genes from a mouse pool (A) *Alas1*, (B) *Alad*, (C) *Uros*, (D) *Fech* from FXR Atlas (<https://fxratlas.tugraz.at/?#>).^[42] Abbreviations: ALAD, aminolevulinic acid dehydratase; FECH, ferrochelatase; FXR, farnesoid X receptor.

in vitro models, we observed increased expression in human *ALAS1*, which confirms a previous report demonstrating that h*ALAS1* is regulated by FXR.^[22] In addition, OCA also increased *UROS* and *FECH* expression (Figure 7A, B, D–F, H) but not expression of

uroporphyrinogen III decarboxylase (*UROD*) (Figure 7C, G) in both human cell types. Furthermore, knockdown of *FXR* in HepG2 cells did not alter expression of heme biosynthetic genes *ALAS1*, *UROS*, *UROD*, or *FECH*, supporting that primarily activation of FXR alters the

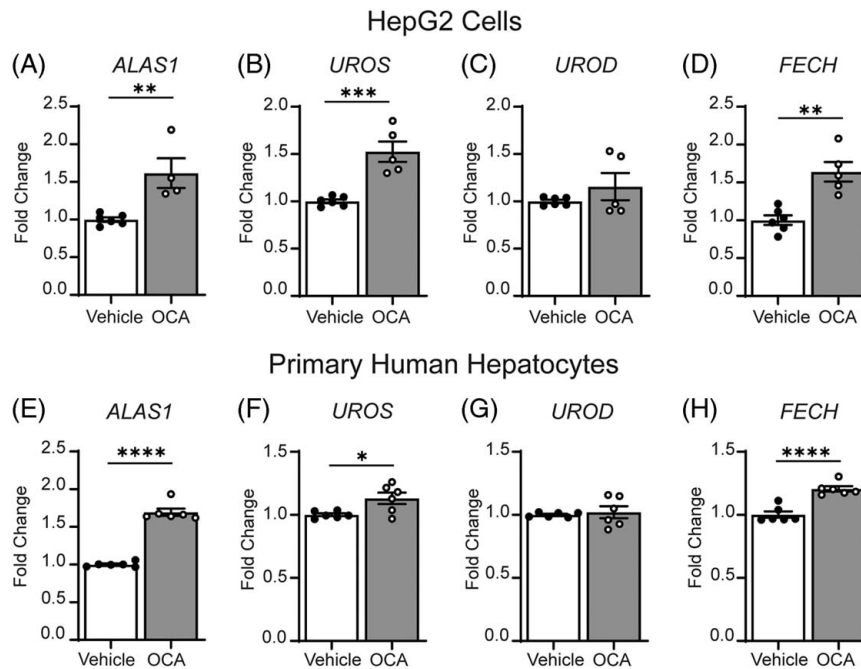


FIGURE 7 Activation of FXR in HepG2 and primary human hepatocytes results in alterations in heme biosynthetic genes. (A–D) RNA expression of heme biosynthetic genes (A) *ALAS1*, (B) *UROS*, (C) *UROD*, (D) *FECH* from HepG2 cells treated with vehicle or 100 nM OCA for 24 h. (E–H) Expression of heme biosynthetic genes from primary human hepatocytes treated with vehicle or 100 nM OCA for 24 h. $n = 4–6$; mean \pm SEM; samples per group, and statistical analysis was completed using an unpaired *t* test, $p < 0.05$. * $p < 0.05$, ** $p < 0.01$, *** $p < 0.001$, **** $p < 0.0001$. Abbreviations: *ALAS1*, aminolevulinic acid synthase 1; *FECH*, ferrochelatase; OCA, obeticholic acid; *UROD*, uroporphyrinogen III decarboxylase.

expression of human heme biosynthetic genes (Supplemental Figure S11A–D, <http://links.lww.com/HC9/A433>). Taken together, activation of FXR by OCA appears to increase expression of multiple heme synthesis genes in human *in vitro* models, demonstrating that FXR may play a role in regulating multiple enzymes in the synthesis of heme in humans, not just *ALAS1*.

DISCUSSION

Most patients with EPP have protoporphyrin accumulation in the skin causing light sensitivity. However, in up to 20% of the patients, protoporphyrin accumulates in the liver, with ~5%–10% of EPP patients developing severe liver injury noted by porphyrin-containing bile plugs and ductular reaction.^[3]

Bile acids have been linked to heme biosynthesis and treatment of EPP patients and have also been recapitulated in rodent models,^[23,24] suggesting that bile acid-induced choleresis and/or bile acid signaling may reduce porphyrin accumulation in the liver. Furthermore, intermediates of bile acid synthesis have been shown to regulate heme biosynthesis.^[25] Based on this information and our study confirming the results from Fickert et al,^[31] we examined if and how the bile acid-related nuclear receptor, FXR, relates to protoporphyrin accumulation and the resulting ductular reaction in the injured liver.

Tissue accumulation of protoporphyrin is a symptom of EPP (*FECH* loss-of-function mutations) and X-linked protoporphyria (XLP, *ALAS2* gain-of-function mutations).^[47] DDC treatment in mice results in liver protoporphyrin accumulation in both sexes, thus mimicking EPP, which exhibits similar incidence in females and males^[47] unlike XLP. Female *Fxr*KO livers exhibited a robust reduction in *Fech* gene expression compared to male mice; therefore, here we focused on the female response. Nonetheless, our data for male *Fxr*KO mice are similar to the previously published study by Fickert et al.^[31] In this study, we confirmed that both male and female *Fxr*KO mice have reduced bile plugs and ductular reaction formation when treated with DDC, which validates previous results.^[31] Furthermore, we showed that bile plug formation and the subsequent ductular reaction are dependent on FXR in the hepatocyte but not in the intestine. *Shp* is a downstream target of FXR. Previous literature has shown exacerbated bile plug formation and ductular reaction when *Shp* is absent in the hepatocyte.^[48] Taken together, these findings highlight the role of FXR in bile plug development and the resulting ductular reaction.

The bile plugs from DDC treatment can contain protoporphyrin, and we confirmed that the livers in the global *Fxr*KO mice had less porphyrin accumulation. Although we observed significant differences in porphyrin accumulation in the liver between the female WT and *Fxr*KO mice, heme levels were unperturbed. Based

on these data we conjecture that loss of FXR may cause reduction in protoporphyrin accumulation but not influence the heme pool in female livers. However, in male mice, we found that although heme in the liver was similar in both genotypes at basal levels, upon DDC diet, heme in the liver increased to a greater extent in WT mice compared with the *Fxr*KO mice. We also noted that in male mice only, *Hmox1*, the rate-limiting step of heme catabolism, was elevated in WT mice with DDC treatment, but this elevation was not observed in *Fxr*KO mice. This suggests sexual differences in mechanisms that are employed by FXR to link heme biosynthesis to ductular reaction.

Cytochrome p450s, in particular the CYP3A family, play a role in the metabolism of DDC.^[27,38,39] Our data showed increased *Cyp3a11* transcript expression in both sexes and genotypes in response to DDC; therefore, we do not expect aberrant DDC metabolism to be the cause of decreased bile plug and ductular reaction formation in the *Fxr*KO mice.

In the female global *Fxr*KO mice, we saw significantly reduced basal *Alad* and *Fech* expression, which was not further decreased upon DDC treatment. Similar findings were noted for ALAD protein expression but not for FECH.

We mined the FXR Atlas ChIP-Seq database of pooled samples from multiple murine studies in the liver (<https://fxratlas.tugraz.at/?#>)^[42] and identified binding peaks for both *Alad* and *Fech*. These results indicate that FXR can bind and directly regulate genes in the heme biosynthetic pathway. A caveat to this result is that the mouse pooled data came from studies in male mice only. We tested the female liver samples from the current mouse study and failed to observe alteration in FXR recruitment to heme biosynthetic genes in our female liver samples. It is possible that since we focused only on one region, we missed the regions that could be more relevant for FXR binding. It is also possible that in female livers FXR may be acting indirectly to regulate these heme biosynthetic genes. For example, PCG1 α , FOXO1, NRF1, and Rev-erb α/β can regulate the rate-limiting step in the liver, *Alas1*.^[43–45] Basal reductions in *Ppargc1a* and *Foxo1* mimic the decreases *Alad* and *Fech* in female mice, indicating that the reductions in PGC1 α transcript may result in reduced heme synthesis genes when FXR is absent.

ALAS1, the rate-limiting step of heme biosynthesis, is regulated by human FXR but not in mice as reported previously.^[22] We confirm this in our *in vitro* HepG2 and primary human hepatocyte models that *ALAS1* expression is increased by FXR agonism with OCA treatment along with other heme biosynthetic genes, *Alad* and *Fech*. In addition, pregnane X receptor and constitutive androstane receptor activation has also been shown to regulate *Alas1/2* expression,^[49] while PGC1 α ^[44] and Rev-erb α/β ^[45] can modulate the circadian pattern of *Alas1*. Taken together, these studies^[22,44,45,49] suggest

that pregnane X receptor/constitutive androstane receptor and PGC1 α /Rev-erb α/β regulate *Alas1* while FXR and bile acids may regulate *FECH* in mice. Moreover, we also found that human FXR activation can induce expression of heme biosynthetic genes, supporting our findings from the mouse model that FXR can have a regulatory role in the expression of heme biosynthetic genes.

Our striking observations that loss of murine FXR reduces porphyrin accumulation and the subsequent ductular reaction upon DDC treatment underscore the significance of understanding and modulating FXR activity in EPP patients. Since FXR activity appears to determine pathomorphological changes in the liver, investigation into the antagonism of FXR with clinically available medications, such as ursodeoxycholic acid, a naturally occurring bile acid,^[50] may be advantageous in EPP patients with liver disease.

While this study uncovered some interesting findings, there were some limitations. First, we did not show direct FXR regulation of target heme biosynthetic genes and only showed expression changes and ChIP-seq/qPCR data. We also did not treat WT mice with a FXR antagonist under DDC treatment to see if we can phenocopy the findings of our genetic knockout mouse model. Despite these limitations, we demonstrate that the expression pattern of multiple genes in the heme biosynthesis pathway change in the presence and absence of FXR. In conclusion, we uncover that loss of FXR, specifically in the hepatocyte, results in reduced bile plug formation and subsequent ductular reaction, and that these data may be clinically relevant to EPP patients and open new strategies of FXR modulation for more treatment options for these patients.

FUNDING INFORMATION

NIDDK R01-113080, American Cancer Society, RSG132640; Margin of Excellence Award, Division of Nutritional Sciences, University of Illinois-Urbana-Champaign.

CONFLICTS OF INTEREST

The authors have no conflicts to report.

ORCID

Angela E. Dean  <https://orcid.org/0000-0002-9141-2590>

Martin Wagner  <https://orcid.org/0000-0002-2769-2364>

REFERENCES

1. Boyer JL. Bile formation and secretion. *Compr Physiol*. 2013;3:1035–78.
2. Gouw ASH, Clouston AD, Theise ND. Ductular reactions in human liver: diversity at the interface. *Hepatology*. 2011;54:1853–63.
3. Bloomer JR. The liver in protoporphyria. *Hepatology*. 1988;8:402–7.

4. Gross U, Frank M, Doss MO. Hepatic complications of erythropoietic protoporphyria. *Photodermatol Photoimmunol Photomed*. 1998;14:52–7.
5. Holme SA, Worwood M, Anstey AV, Elder GH, Badminton MN. Erythropoiesis and iron metabolism in dominant erythropoietic protoporphyria. *Blood*. 2007;110:4108–10.
6. Magnus IA, Jarrett A, Prankerd TA, Rimington C. Erythropoietic protoporphyria. A new porphyria syndrome with solar urticaria due to protoporphyriaemia. *Lancet*. 1961;2:448–51.
7. Todd DJ. Erythropoietic protoporphyria. *Br J Dermatol*. 1994;131:751–66.
8. Ajioka RS, Phillips JD, Kushner JP. Biosynthesis of heme in mammals. *Biochim Biophys Acta*. 2006;1763:723–36.
9. Wang B, Rudnick S, Cengia B, Bonkovsky HL. Acute hepatic porphyrias: review and recent progress. *Hepatol Commun*. 2019;3:193–206.
10. Boulechfar S, Lamoril J, Montagutelli X, Guenet JL, Deybach JC, Nordmann Y, et al. Ferrochelatase structural mutant (Fechm1-Pas) in the house mouse. *Genomics*. 1993;16:645–8.
11. Davies R, Schuurman A, Barker CR, Clothier B, Chernova T, Higginson FM, et al. Hepatic gene expression in protoporphyric fech mice is associated with cholestatic injury but not a marked depletion of the heme regulatory pool. *Am J Pathol*. 2005;166:1041–53.
12. Tutois S, Montagutelli X, Da Silva V, Jouault H, Rouyer-Fessard P, Leroy-Viard K, et al. Erythropoietic protoporphyria in the house mouse. A recessive inherited ferrochelatase deficiency with anemia, photosensitivity, and liver disease. *J Clin Invest*. 1991;88:1730–6.
13. Makishima M. Identification of a nuclear receptor for bile acids. *Science*. 1999;284:1362–5.
14. Parks DJ. Bile acids: natural ligands for an orphan nuclear receptor. *Science*. 1999;284:1365–8.
15. Sinal CJ, Tohkin M, Miyata M, Ward JM, Lambert G, Gonzalez FJ. Targeted disruption of the nuclear receptor FXR/BAR impairs bile acid and lipid homeostasis. *Cell*. 2000;102:731–44.
16. Wang H, Chen J, Hollister K, Sowers LC, Forman BM. Endogenous bile acids are ligands for the nuclear receptor FXR/BAR. *Mol Cell*. 1999;3:543–3.
17. Duran-Sandoval D, Mautino G, Martin G, Percevault F, Barbier O, Fruchart J-C, et al. Glucose regulates the expression of the farnesoid X receptor in liver. *Diabetes*. 2004;53:890–8.
18. Ma K, Saha PK, Chan L, Moore DD. Farnesoid X receptor is essential for normal glucose homeostasis. *J Clin Invest*. 2006;116:1102–9.
19. Renga B, Mencarelli A, D'Amore C, Cipriani S, Baldelli F, Zampella A, et al. Glucocorticoid receptor mediates the gluconeogenic activity of the farnesoid X receptor in the fasting condition. *FASEB J*. 2012;26:3021–1.
20. Stayrook KR, Bramlett KS, Savkur RS, Ficorilli J, Cook T, Christe ME, et al. Regulation of carbohydrate metabolism by the farnesoid X receptor. *Endocrinology*. 2005;146:984–91.
21. Watanabe M, Houten SM, Wang L, Moschetta A, Mangelsdorf DJ, Heyman RA, et al. Bile acids lower triglyceride levels via a pathway involving FXR, SHP, and SREBP-1c. *J Clin Invest*. 2004;113:1408–8.
22. Peyer A-K, Jung D, Beer M, Gnerre C, Keogh A, Stroka D, et al. Regulation of human liver δ -aminolevulinic acid synthase by bile acids. *Hepatology*. 2007;46:1960–70.
23. Berenson MM, Marin JGG, Larsen R, Avner D. Effect of bile acids on hepatic protoporphyrin metabolism in perfused rat liver. *Gastroenterology*. 1987;93:1086–93.
24. Van Hattum J, Baart de la Faille H, Van den Berg JW, Edixhoven-Bosdijk A, Wilson JH. Chenodeoxycholic acid therapy in erythrohepatic protoporphyria. *J Hepatol*. 1986;3:407–12.
25. Javitt NB, Rifkind A, Kappas A. Porphyrin-heme pathway: regulation by intermediates in bile acid synthesis. *Science*. 1973;182:841–2.
26. Clerbaux L-A, Hul NV, Gouw ASH, Manco R, Español-Suñer R, Leclercq IA. Relevance of the CDE and DDC mouse models to study ductular reaction in chronic human liver diseases. In: Bartholomew I, ed. *Experimental Animal Models of Human Diseases – An Effective Therapeutic Strategy*. InTech. Epub ahead of print; May 23, 2018. doi: 10.5772/intechopen.69533
27. Fickert P, Stöger U, Fuchsbichler A, Moustafa T, Marschall H-U, Weiglein AH, et al. A new xenobiotic-induced mouse model of sclerosing cholangitis and biliary fibrosis. *Am J Pathol*. 2007;171:525–36.
28. Pose E, Sancho-Bru P, Coll M. 3,5-diethoxycarbonyl-1, 4-dihydrocollidine diet: A rodent model in cholestasis research. In: Vinken M, ed. *Experimental Cholestasis Research*. Springer. 249–57.
29. Solomon HM, Figge FHJ. Porphyrin metabolism in mice following quantitative administration of collidine compounds and oxidation products. *Proc Soc Exp Biol Med*. 1960;105:484–85.
30. Solomon HM, Figge FHJ. Disturbance in porphyrin metabolism caused by feeding diethyl 1, 4-dihydro-2, 4, 6-trimethylpyridine-3, 5-dicarboxylate. *Proc Soc Exp Biol Med*. 1959;100:583–6.
31. Fickert P, Fuchsbichler A, Moustafa T, Wagner M, Zollner G, Hallibasic E, et al. Farnesoid X receptor critically determines the fibrotic response in mice but is expressed to a low extent in human hepatic stellate cells and periductal myofibroblasts. *Am J Pathol*. 2009;175:2392–405.
32. Stedman C, Liddle C, Coulter S, Sonoda J, Alvarez JG, Evans RM, et al. Benefit of farnesoid X receptor inhibition in obstructive cholestasis. *Proc Natl Acad Sci*. 2006;103:11323–8.
33. Livak KJ, Schmittgen TD. Analysis of relative gene expression data using real-time quantitative PCR and the 2(-Delta Delta C (T)) method. *Methods*. 2001;25:402–8.
34. Ballatori N, Christian WV, Lee JY, Dawson PA, Soroka CJ, Boyer JL, et al. OST α -OST β : A major basolateral bile acid and steroid transporter in human intestinal, renal, and biliary epithelia. *Hepatology*. 2005;42:1270–9.
35. Boyer JL, Trauner M, Mennone A, Soroka CJ, Cai S-Y, Moustafa T, et al. Upregulation of a basolateral FXR-dependent bile acid efflux transporter OST α -OST β in cholestasis in humans and rodents. *Am J Physiol Gastrointest Liver Physiol*. 2006;290:G1124–30.
36. Goodwin B, Jones SA, Price RR, Watson MA, McKee DD, Moore LB, et al. A regulatory cascade of the nuclear receptors FXR, SHP-1, and LXR-1 represses bile acid biosynthesis. *Mol Cell*. 2000;6:517–26.
37. Lu TT, Makishima M, Repa JJ, Schoonjans K, Kerr TA, Auwerx J, et al. Molecular basis for feedback regulation of bile acid synthesis by nuclear receptors. *Mol Cell*. 2000;6:507–15.
38. Hanada S, Snider NT, Brunt EM, Hollenberg PF, Omary MB. Gender dimorphic formation of mouse Mallory-Denk bodies and the role of xenobiotic metabolism and oxidative stress. *Gastroenterology*. 2010;138:1607–7.
39. Saggi H, Maitra D, Jiang A, Zhang R, Wang P, Cornuet P, et al. Loss of hepatocyte β -catenin protects mice from experimental porphyria-associated liver injury. *J Hepatol*. 2019;70:108–7.
40. Sato K, Marziani M, Meng F, Francis H, Glaser S, Alpini G. Ductular reaction in liver diseases: Pathological mechanisms and translational significances. *Hepatology*. 2019;69:420–30.
41. Jungwirth E, Panzitt K, Marschall H-U, Thallinger GG, Wagner M. Meta-analysis and consolidation of farnesoid X receptor chromatin immunoprecipitation sequencing data across different species and conditions. *Hepatol Commun*. 2021;5:1721–36.
42. Jungwirth E, Panzitt K, Marschall H-U, Thallinger GG. A comprehensive FXR signaling atlas derived from pooled ChIP-seq data. *Stud Health Technol Inform*. 2019;260:105–2.
43. Braidotti G, Borthwick IA, May BK. Identification of regulatory sequences in the gene for 5-aminolevulinic acid synthase from rat. *J Biol Chem*. 1993;268:1109–7.

44. Handschin C, Lin J, Rhee J, Peyer A-K, Chin S, Wu P-H, et al. Nutritional regulation of hepatic heme biosynthesis and porphyria through PGC-1 α . *Cell*. 2005;122:505–15.
45. Raghuram S, Stayrook KR, Huang P, Rogers PM, Nosie AK, McClure DB, et al. Identification of heme as the ligand for the orphan nuclear receptors REV-ERB α and REV-ERB β . *Nat Struct Mol Biol*. 2007;14:1207–3.
46. Bakken AF, Thaler MM, Schmid R. Metabolic regulation of heme catabolism and bilirubin production. I. Hormonal control of hepatic heme oxygenase activity. *J Clin Invest*. 1972;51: 530–6.
47. Balwani M. Erythropoietic protoporphyria and x-linked protoporphyria: Pathophysiology, genetics, clinical manifestations, and management. *Mol Genet Metab*. 2019;128:298–303.
48. Shaw RPH, Kolyvas P, Dang N, Hyon A, Bailey K, Anakk S. Loss of hepatic small heterodimer partner elevates ileal bile acids and alters cell cycle-related genes in male mice. *Endocrinology*. 2022;163:bqac052.
49. Fraser DJ, Zumsteg A, Meyer UA. Nuclear receptors constitutive androstane receptor and pregnane X receptor activate a drug-responsive enhancer of the murine 5-aminolevulinic acid synthase gene. *J Biol Chem*. 2003;278:39392–401.
50. Mueller M, Thorell A, Claudel T, Jha P, Koefeler H, Lackner C, et al. Ursodeoxycholic acid exerts farnesoid X receptor-antagonistic effects on bile acid and lipid metabolism in morbid obesity. *J Hepatol*. 2015;62:1398–404.

How to cite this article: Dean AE, Jungwirth E, Panzitt K, Wagner M, Anakk S. Hepatic farnesoid X receptor is necessary to facilitate ductular reaction and expression of heme biosynthetic genes. *Hepatol Commun*. 2023;7:e0213. <https://doi.org/10.1097/HC9.0000000000000213>